Submission code: VMNDJ8ZWMW

See this and other abstracts on our website: https://home.sbgf.org.br/Pages/resumos.php

Enhancing the Value of Converted-Wave Data through PS Full-Waveform Inversion at Ivar Aasen

Andrew Bullock (SLB), Xin Cheng (SLB), Peng Wang (SLB), Alex Cooke (SLB), Emmanuel Sargoussi (SLB)

Enhancing the Value of Converted-Wave Data through PS Full-Waveform Inversion at Ivar Aasen

Please, do not insert author names in your submission PDF file

Abstract

While the acquisition, processing, and imaging of ocean-bottom data for compressional wave (PP) imaging has taken off in recent years, the full value of the converted waves measured on the horizontal components (PS) is not always exploited. Improved utilisation of PS data relies on the ability to produce more accurate and well-resolved shear velocity models. We apply a new PS-FWI method using single-mode propagators to simulate both P and S waves (Zhai et al. 2024). By applying the Born approximation, P-to-S converted waves are modelled and compared with field data for shear velocity inversion. The technique adapts existing P-wave solvers for S-wave simulation, ensuring computational efficiency and high-quality results. This method promises accurate shear velocity updates with pure P-to-S conversions.

Introduction

While the acquisition, processing, and imaging of ocean-bottom data for compressional wave (PP) imaging has taken off in recent years, the full value of the converted waves measured on the horizontal components (PS) is not always exploited. PS data can deliver additional value by providing complementary constraints for amplitude versus offset (AVO) inversion (Bullock et al. 2019), imaging where gas in the overburden creates seismically obscured areas (Hanson et al. 1999) for complementary structural imaging (Tillotson et al. 2019) and imaging of low p-impedance contrast reservoirs (Bullock et al. 2015). Improved utilisation of PS data relies on the ability to produce more accurate and well-resolved shear velocity models. Recent rapid improvements in PP model building, including elastic full-waveform inversion (EFWI) and compressional velocity (Vp) updates to higher frequencies, have improved the accuracy of the down-going P leg in PS model building, and are enablers for PS-FWI to step up to equivalent shear velocity (Vs) model detail and deliver increased confidence in the PS image.

We apply a new PS-FWI method using single-mode propagators to simulate both P and S waves (Zhai et al. 2024). By applying the Born approximation, P-to-S converted waves are modelled and compared with field data for shear velocity inversion. The technique adapts existing P-wave solvers for S-wave simulation, ensuring computational efficiency and high-quality results. This method promises accurate shear velocity updates with pure P-to-S conversions.

Ivar Aasen Case Study

We successfully applied this method to ocean-bottom cable (OBC) data acquired in 2019 over the Ivar Aasen field in the Norwegian North Sea and in water depths of approximately 120 m. The survey area exhibits complex geological features including shallow channels, high-amplitude thin injected or remobilised sand bodies in the overburden, connected faulting zones, and a high-contrast chalk layer at ~2000 m depth with thinly layered sand reservoirs beneath. These features are observed in both the PP and PS Kirchhoff depth migration (KDM) images

(Figure 1). Input OBC data had a receiver line spacing of 300 m, and a receiver point spacing of 25 m. A mature, anisotropic Vp model derived from FWI to a maximum frequency of 30 Hz was provided.

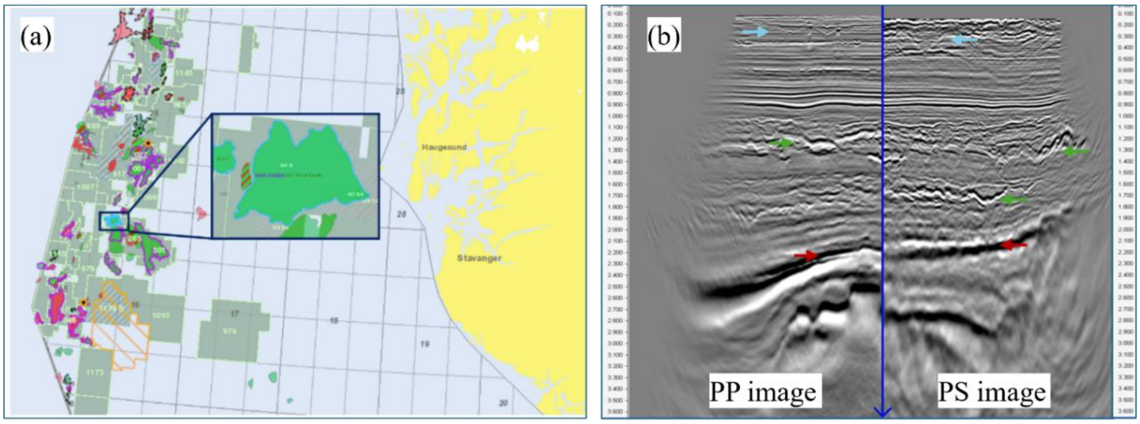

Figure 1 *(a) Location of Ivar Aasen field (modified from https://factmaps.sodir.no/factmaps/3_0) and (b) example PP (left) and PS (right) Kirchhoff depth migration (KDM) images showing characteristic North Sea features such as shallow channels (blue arrows), sand injectites (green arrows), and a chalk layer (red arrows) with thin reservoir sands beneath.*

PS-FWI Workflow

PS signal processing including rotation, demultiple and shear-wave splitting corrections were applied to the supplied data, with additional PS static derivation performed consistent with the Vs model building. Demultiple data were preferred due to the Born approximation made in this formulation of PS-FWI. Data were compensated for Qp and Qs phase effects prior to the model build. Data were split to azimuth sectors for PS tomography with an offset/azimuth borrowing and interpolation scheme applied to ensure bins were fully populated.

A denoised vertical geophone component (Z) was supplied for surface wave inversion to derive a high-resolution near-surface Vs model (Boiero et al. 2013). This model was merged into a deeper initial model determined from Vp/Vs ratios derived at well locations and then extrapolated along key geological structures. The initial Vs model was updated by tomography driven by PP-PS event registration and anisotropy calibration to ensure alignment. This was followed by PP-PS tomography (Bullock et al. 2015) to resolve the low-wavenumber model.

The FWI sequence interleaved two bands of PS-FWI up to 30 Hz with PP-PS tomography to increase the resolution of the Vs model while continuing to maintain accurate kinematics. This workflow increased the resolution of the Vs model and resulted in improved PS imaging with reduced top chalk distortions below the sand injectites and sharper sub-chalk faulting (Figure 2).

Discussion

Application of this PS-FWI workflow has improved the resolution and accuracy of the Vs model compared to a traditional tomographic workflow (Figure 2) and achieved equivalent resolution to the Vp model and PP imaging generated to the same frequency (Figure 3).

PS imaging can deliver a high-quality image to complement existing PP datasets. We show contrasting imaging of injected sands bodies at different levels (Figure 1), faulting within the Grid formation (Figure 3), and coherent PS reflections through the Heimdal interval (Figure 4).

Understanding is further improved when the high-resolution Vs model is combined to derive a detailed Vp/Vs ratio that is consistent with faulting in the Grid formation and shows a low Vp/Vs area sub-chalk (Figure 4).

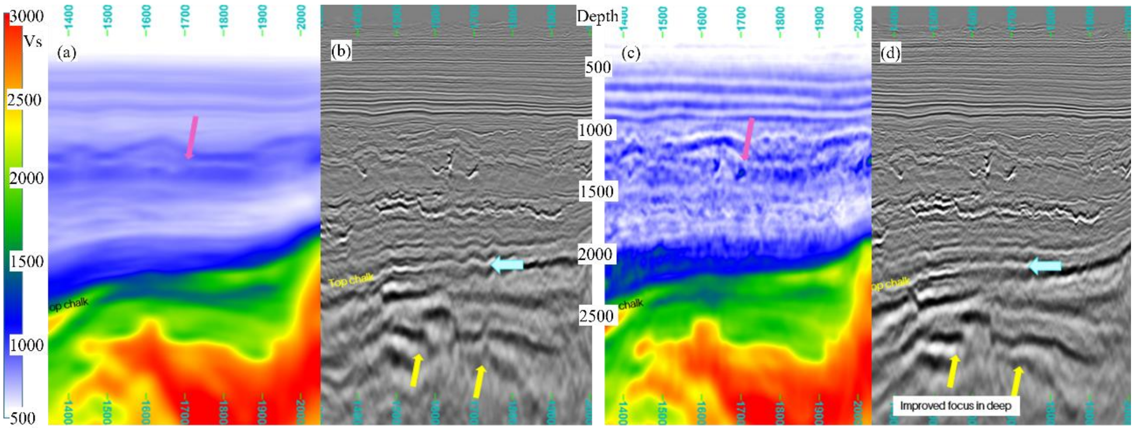

Figure 2 *(a), (b) Vs and PS KDM image for the initial Vs model and (c), (d) after the PS-FWI workflow. Vs velocity details are enhanced by the PS-FWI workflow, including high velocity sand injectites. Distortions to top chalk are reduced following this update (blue arrow), and sub-chalk faulting is sharpened in the PS image (yellow arrows).*

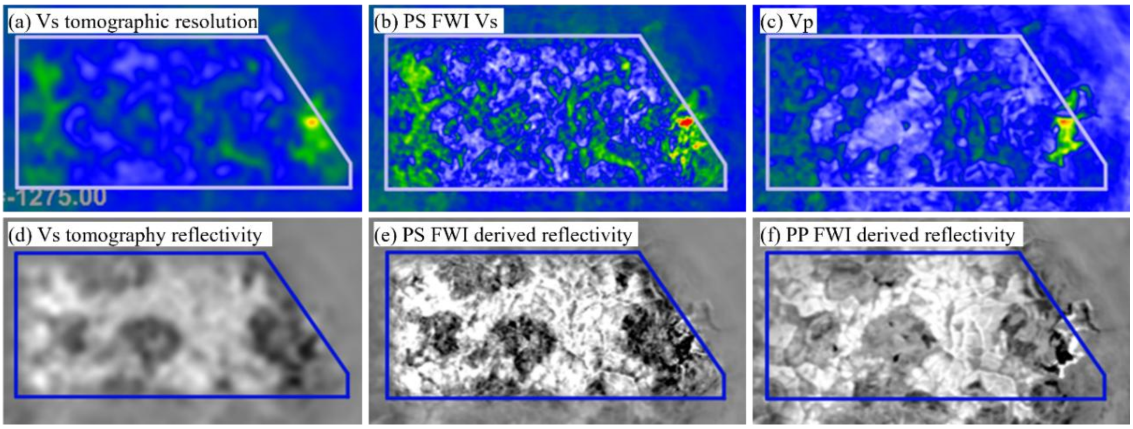

Figure 3 Velocity depth slices through the sand injectite zone at 1275 m depth for (a) Vs with tomographic resolution of ~500 m, (b) Vs after PS FWI workflow with ~50 m wavelength details, and (c) supplied Vp after PP FWI. Equivalent first derivative of the velocity fields are shown in (d-f). PS FWI workflow achieves equivalent levels of detail to PP FWI.

Conclusions

We implemented a new PS-FWI method up to 30 Hz on OBC data from the Ivar Aasen field to achieve high wavenumber Vs updates. PS imaging complements the PP data, showing a characteristic imaging response for layers above the chalk. The detailed Vs model, Vp/Vs ratio and PS-FWI derived reflectivity have a resolution equivalent to Vp and may be used to assist interpretation and better constrain the estimate of elastic and petrophysical parameters.

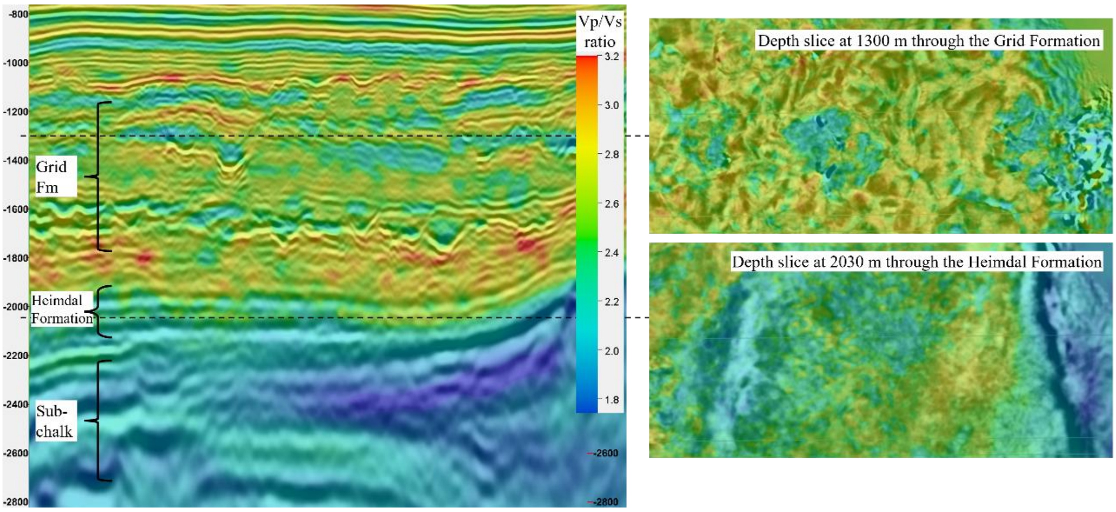

Figure 4 *Detailed Vp/Vs ratio attribute is well correlated with stratigraphic intervals, and seen on depth slices through the polygonal faulting of the Grid Formation and the Heimdal formation. Seismic shown is the PS KDM.*

Acknowledgments

The authors thank the Ivar Aasen license operator Aker BP and the partners Equinor, DNO, OKEA, and M Vest Energy for their permission to publish this data example. We thank SLB and colleagues for support, advice and encouragement throughout the project.

References

Boiero, D., Wiarda, E., and Vermeer, P. [2013] Surface- and guided-wave inversion for near-surface modelling in land and shallow marine seismic data. The Leading Edge, 32, 638–646.

Bullock, A., Aviles, J., Leone, C. and Butt, J. [2019]. Converted wave amplitude versus offset (AVO) QC and joint PP-PS density inversion at Clair Ridge. 81st EAGE Conference and Exhibition, Extended Abstracts.

Bullock, A., Bekhtin, Y., Ortin, M., Mathewson, J., Henneberg, K. and Saebo, A. [2015]. Improved imaging with PP-PS simultaneous joint tomography over the Grane field. SEG Technical Program Expanded Abstracts, 2094-2097. doi: 10.1190/segam2015-5908890.1.

Hanson, R., MacLeod, M., Bell, C., Thompson, C. and Somod, J. [1999]. Multi-component seismic interpretation: Data integration issues, Alba Field, North Sea. SEG Technical Program Expanded Abstracts, 808-811.

Tillotson, P., Davies, D., Ball, M., and Smith, L. [2019]. Clair Ridge: Learnings from processing the densest ocean bottom node (OBN) survey in the UKCS. 81st EAGE Conference and Exhibition, 2019(1), 1-5.

Zhai, Y., Xu, J., Rickett, J., Wang, P., Cheng, X., Vigh, D., Chen, S. and Smith, C. [2024]. PS reflection-based full-waveform inversion using single-mode propagator. SEG Technical Program, Expanded Abstracts.